A Triradical-Containing Trinuclear Pd(II) Complex: Spin-Polarized Electronic Transmission, Analog Resistive Switching and Neuromorphic Advancements

Prasenjit Sarkar†[1], Litty Thomas Manamel†[2], Puranjay Saha†[2], Chinmay Jana[1], Amrit Sarmah[3,4], Kannan Udaya Mohanan[5], Bikas C. Das*[2], and Chandan Mukherjee*[1]

[1] Department of Chemistry, Indian Institute of Technology Guwahati, Guwahati, 781039, Assam, India

[2] eNDR Laboratory, School of Physics, IISER Thiruvananthapuram, Vithura, Trivandrum 695551, Kerala, India

[3] Department of Molecular Modelling, Institute of Organic Chemistry and Biochemistry ASCR, v.v.i. Flemingovo nám. 2, CZ-166 10 Prague 6, Czech Republic

[4] Regional Centre of Advanced Technologies and Materials, Faculty of Science, Palacký University Olomouc, 78371 Olomouc, Czech Republic

[5] School of Electrical Engineering and Computer Science, University of Ottawa, Ottawa, ON K1N 6N5, Canada

Corresponding Authors:

*1 Prof. Chandan Mukherjee, E-mail: cmukherjee@iitg.ac.in

*2 Bikas C. Das, Email: bikas@iisertvm.ac.in

† Authors contributed equally to this work.

ORCID iDs

Chandan Mukherjee: https://orcid.org/0000-0002-2771-2468

Bikas C Das: https://orcid.org/0000-0002-4750-0542

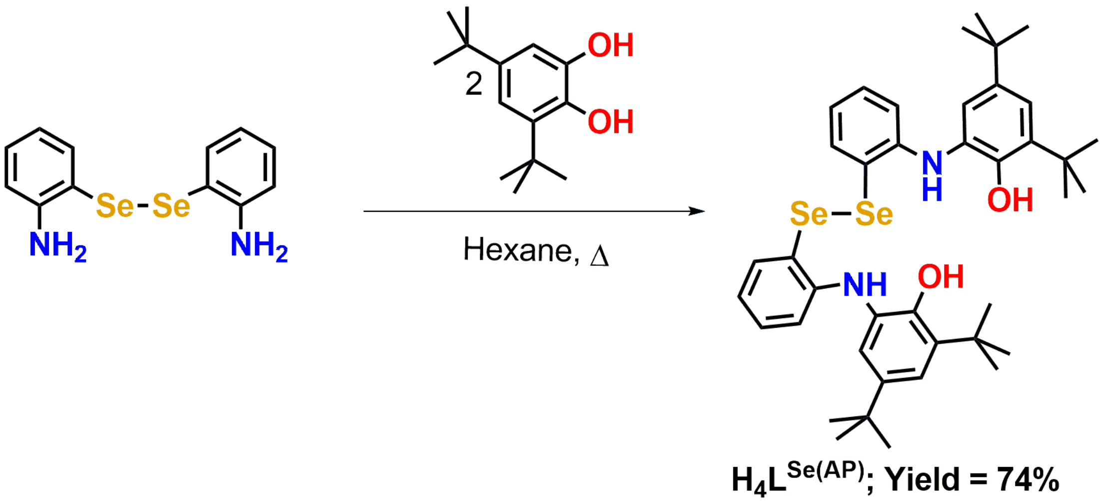

Scheme 1. Synthesis route to the ligand.

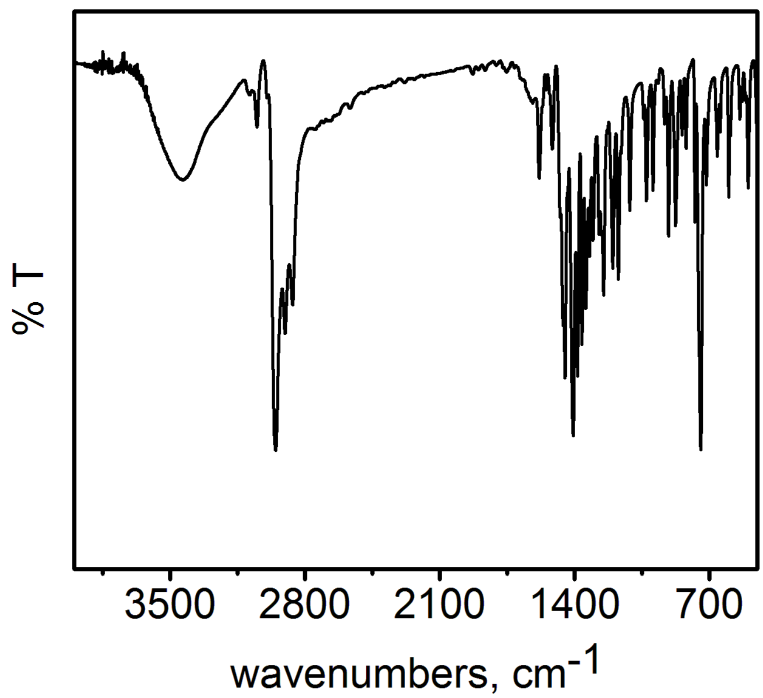

Figure S1. Infrared spectrum of complex **1**.

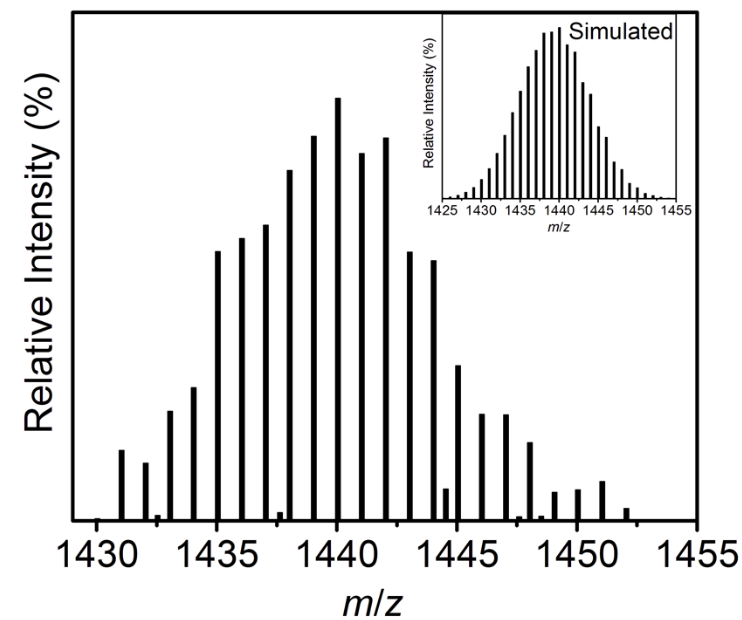

Figure S2. Experimental and simulated mass spectra for complex **1** = $[C_{60}H_{72}N_3O_3Se_3Pd_3 + H]^+$ have been shown.

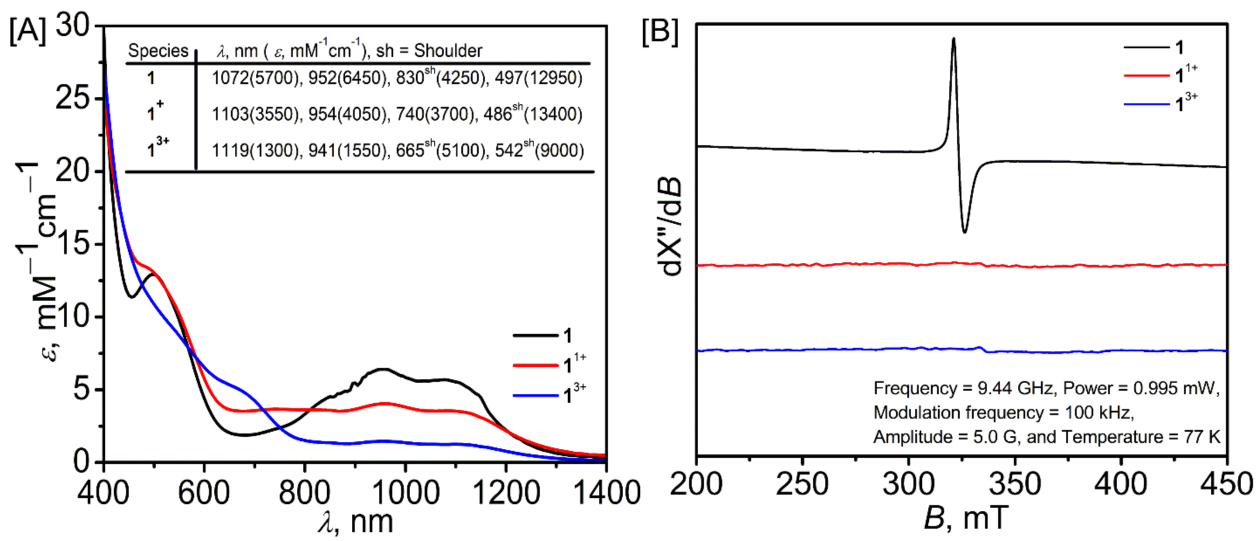

Figure S3. [A]: UV-vis-NIR spectra of complex **1** and its one- and three-electron oxidized species at room temperature in CH_2Cl_2 and [B] X-band EPR spectra for the species in CH_2Cl_2.

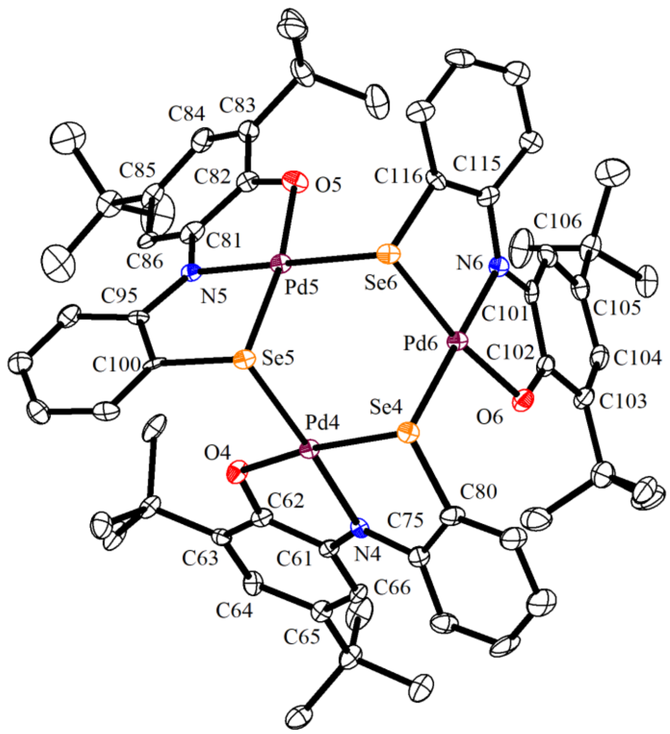

Figure S4. ORTEP diagram of complex **1** (one unit) at 40% probability level. (H atoms are omitted for clarity.

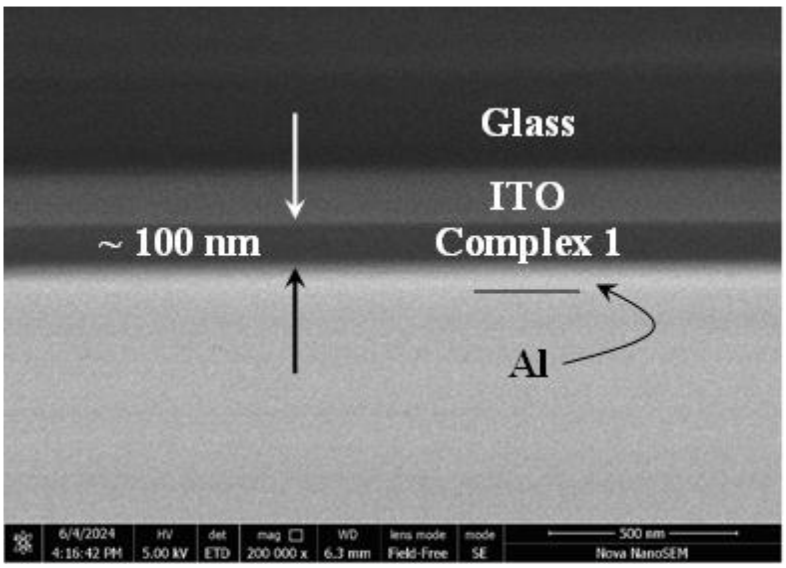

Figure S5. The cross-sectional SEM image of ITO/complex **1**/Al cross-bar memristor device with an average active layer thickness of about 100 nm.

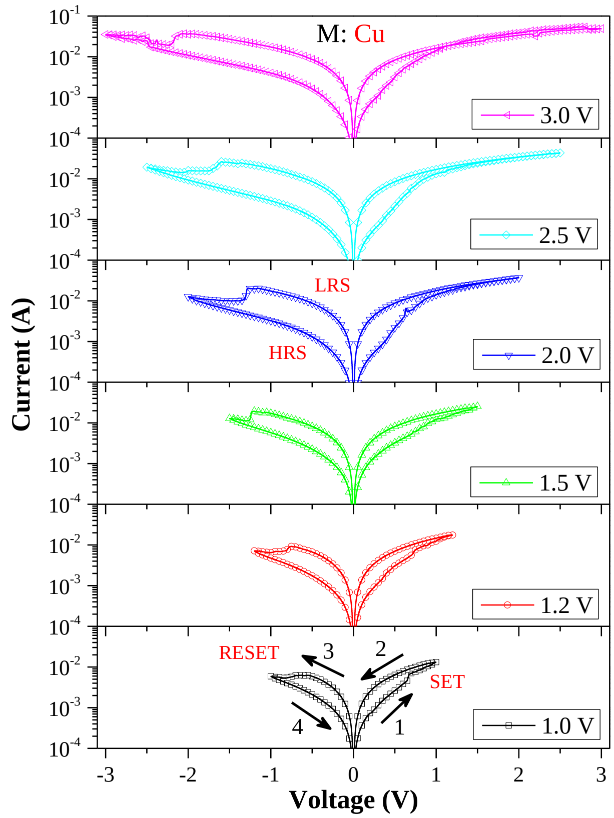

Figure S6. *I*-*V* sweeps in a loop of varying ± V_{max} showing distinct I_{On} (low resistive state, LRS) and I_{Off} (high resistive state, HRS).

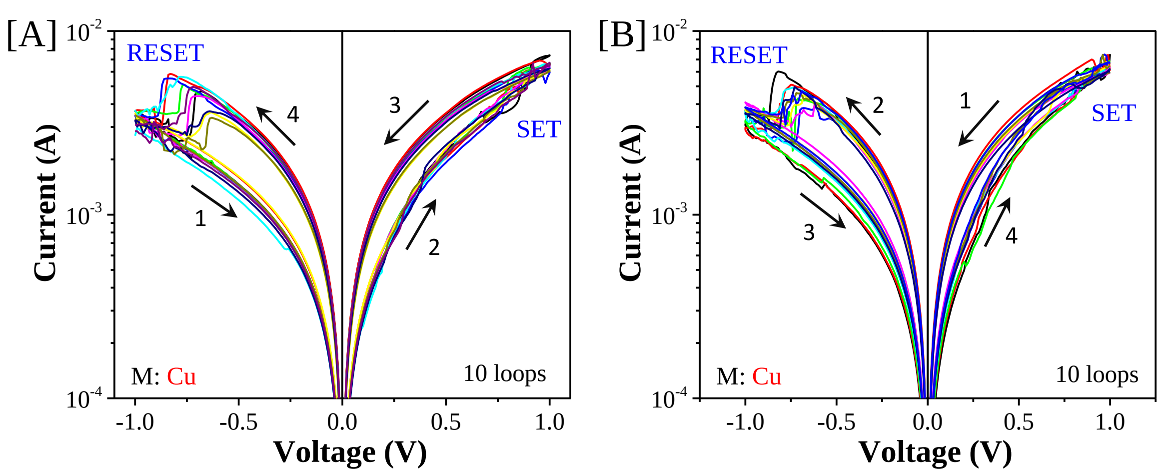

Figure S7. [A and B] *I*-*V* characteristics in 10 consecutive loops in positive (–1.0 V to + 1.0 V) and negative (+ 1.0 V to – 1.0 V) bias sweep direction, respectively.

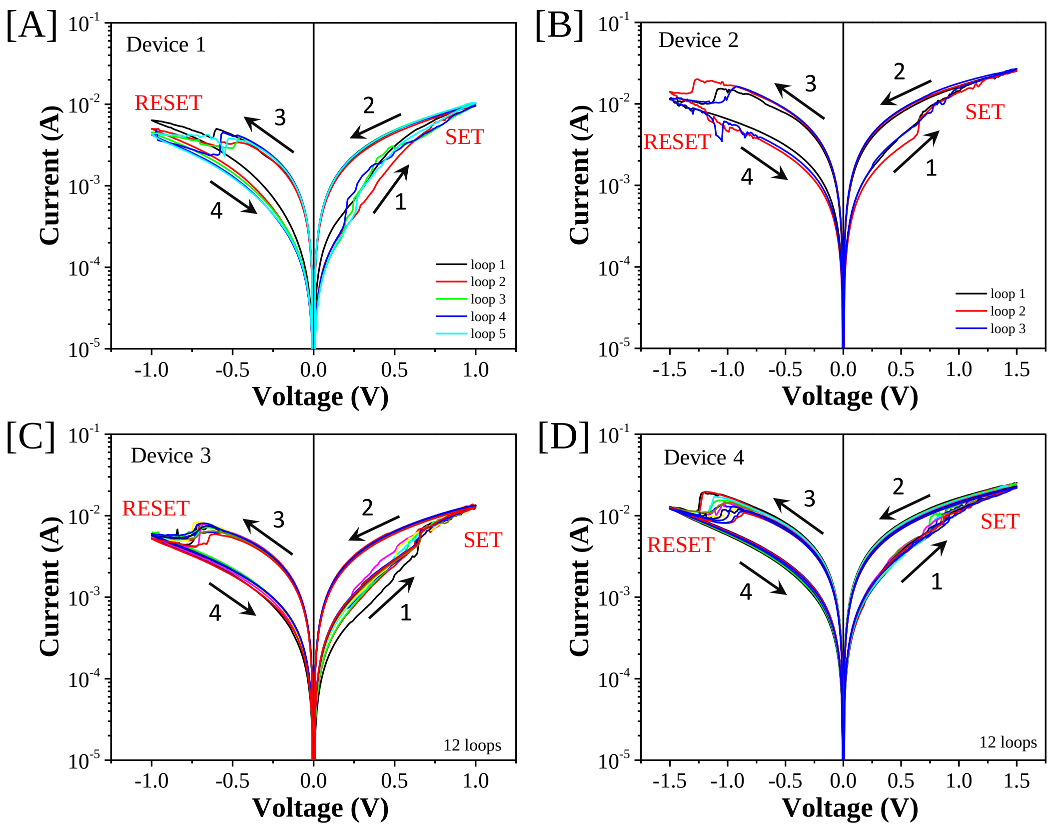

Figure S8. [A - D] *I-V* characteristics in multiple loops for four different devices arbitrarily picked from the 16 fabricated devices.

Section S1:

We performed various control experiments to establish the robustness of our complex **1** for showing resistive switching properties and relevant ReRAM performance. Figures S7 [A] and S7[B] represent *I-V* curves in 10 consecutive loops between ± 1.0 V for the ITO/(complex **1**:PMMA)/Cu device in sweep direction –1.0 V to + 1.0 V (positive) and + 1.0 V to – 1.0 V (negative), respectively. These results unambiguously depict the sweeping direction independent RS property of complex **1**. Next, we have recorded *I-V* curves in multiple loops for four arbitrarily picked devices from 16 devices by sweeping voltage starting from 0 V to $+V_{\text{max}}$ to $-V_{\text{max}}$ to 0 V again as illustrated in Figure S8 [A–D]. Note that V_{max} is considered as 1.0 V (for devices 1 and 3) or 1.5 V (for devices 2 and 4). Interestingly, all the *I-V* curves look very consistent for gradual transformation from the HRS to LRS with the increase of bias towards positive polarity, which is known as the SET process. The RESET process is observed in the negative polarity of applied bias voltage transiting from the LRS to HRS with a negative differential resistance (NDR) peak. Therefore, the complex **1** molecule robustly displayed the stable memristor property independent of the top metal electrode (Al or Cu), voltage sweep directions, and number of cycles. Eventually, the memristor performance is quite stable in cycle-to-cycle and device-to-device variation. Not only that, we can claim the consistency of the RS property of complex **1** in different batches of device fabrication too.

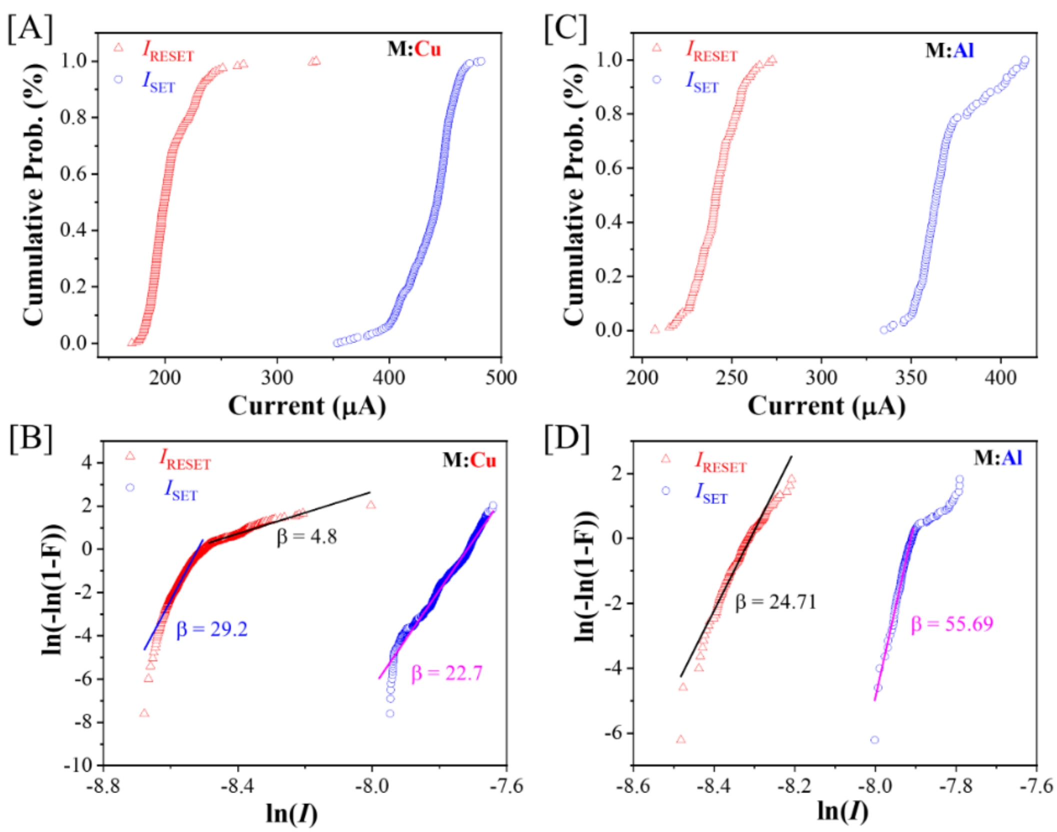

Figure S9. [A and B] Cumulative probability plots of I_{SET} and I_{RESET} currents measured over 1300 cycles for the Cu top electrode device and 550 cycles for the Al top electrode device, respectively. [C and D] Weibull distribution plots of I_{SET} and I_{RESET} currents corresponding to the data in [A and B], respectively.

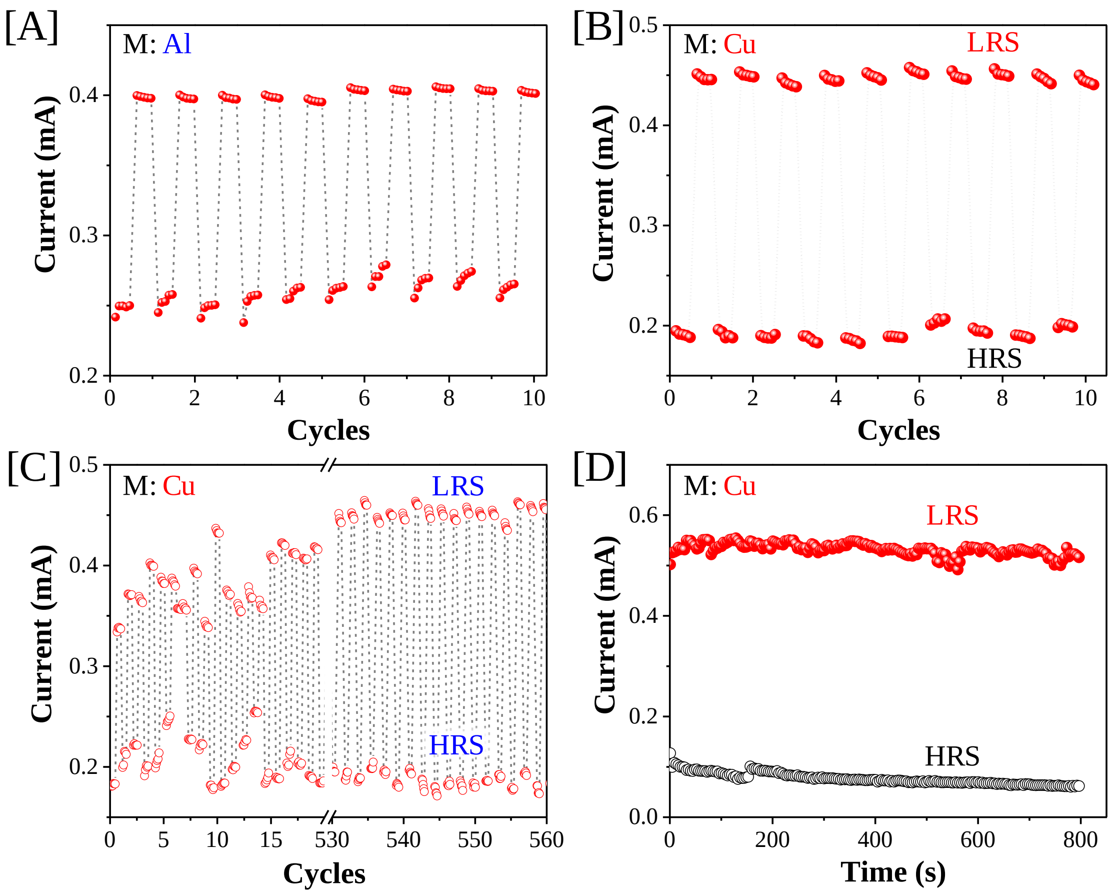

Figure S10. [A] ReRAM application for 10 W/R/E/R cycles for the ITO/(complex **1**:PMMA)/Al device. [C - D] ReRAM, endurance of 560 cycles, and retention of states (HRS and LRS) for more than 800 s, respectively, for the ITO/(complex **1**:PMMA)/Cu device.

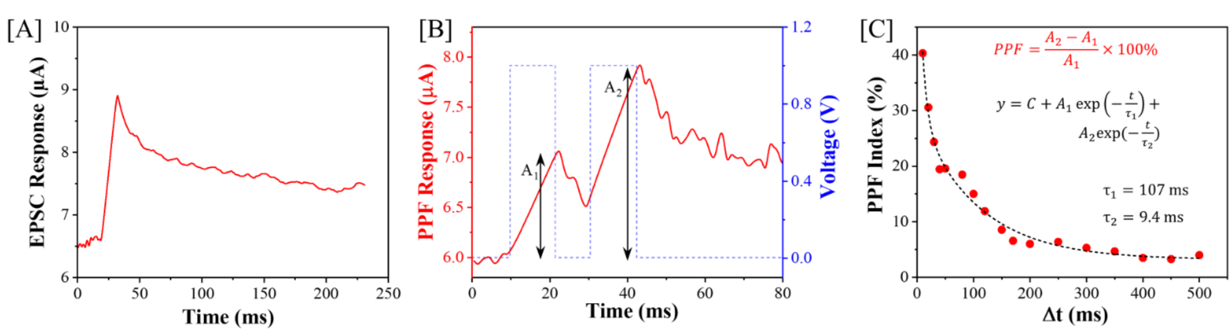

Figure S11. [A] EPSC response was recorded using read pulses of +0.1 V, 1 ms with 1 ms intervals, after applying a pre-synaptic pulse of +1.0 V, 10 ms. [B] A paired-pulse (+1.0 V, 10 ms) with a 10 ms interval was applied to the pre-synaptic terminal (blue dashed line), and the paired-pulse facilitation (PPF) response (red solid line) was recorded at the post-synaptic terminal using read voltage pulses of +0.1 V, 1ms with 1 ms intervals. [C] The PPF index was plotted against varying time intervals (Δ*t*) between the paired pulses applied to the pre-synaptic terminal.

Table S1: Selected bond distances(Å) and bond angles (°) of complex **1**.

Atoms	Experimental	Calculated	Atoms	Experimental	Calculated
Pd4–N4	2.007(4)	2.039	C102–O6	1.302(7)	1.309
Pd4–O4	2.036(3)	2.087	C61–C62	1.433(8)	1.459
Pd4–Se4	2.3587(7)	2.465	C62–C63	1.444(7)	1.441
Pd4–Se5	2.4061(7)	2.500	C63–C64	1.372(8)	1.391
Pd5–N5	2.011(4)	2.040	C64–C65	1.424(8)	1.429
Pd5–O5	2.043(4)	2.087	C65–C66	1.364(7)	1.388
Pd5–Se5	2.3527(7)	2.464	C66–C61	1.427(7)	1.421
Pd5–Se6	2.4080(7)	2.501	C81–C82	1.448(8)	1.460
Pd6–N6	1.993(4)	2.040	C82–C83	1.436(7)	1.441
Pd6–O6	2.038(4)	2.086	C83–C84	1.346(8)	1.391
Pd6–Se6	2.3678(7)	2.462	C84–C85	1.436(8)	1.429
Pd6–Se4	2.4099(7)	2.499	C85–C86	1.361(8)	1.388
C80–Se4	1.933(6)	1.971	C86–C81	1.421(7)	1.421
C100–Se5	1.925(6)	1.971	C101–C102	1.452(8)	1.459
C116–Se6	1.935(6)	1.972	C102–C103	1.444(8)	1.441
C61–N4	1.381(6)	1.377	C103–C104	1.370(8)	1.391
C81–N5	1.368(7)	1.376	C104–C105	1.412(8)	1.429
C101–N6	1.352(7)	1.377	C105–C106	1.363(8)	1.389
C62–O4	1.310(6)	1.309	C106–C101	1.417(8)	1.421
C82–O5	1.301(6)	1.308			
Se4–Pd4–Se5	92.89(2)	95.11	N5–Pd5–Se5	87.89(12)	87.12
O4–Pd4–Se5	97.54(11)	96.87	N5–Pd5–Se6	179.19(13)	176.94
O4–Pd4–Se4	168.87(11)	167.92	N5–Pd5–O5	81.81(16	80.93
N4–Pd4–Se5	176.49(12)	177.58	S6–Pd6–Se4	94.00(2)	95.14
N4–Pd4–O4	81.78(16)	80.93	O6–Pd6–Se6	168.78(11)	168.12
N4–Pd4–Se4	88.04(12)	87.11	O6–Pd6–Se4	97.18(11)	96.69
Se5–Pd5–Se6	92.42(2)	95.14	N6–Pd6–Se6	87.12(14)	87.22
O5–Pd5–Se5	169.56(11)	168.03	N6–Pd6–Se4	178.86(14)	176.96
O5–Pd5–Se6	97.99(11)	96.77	N6–Pd6–O6	81.70(17)	80.97

Table S2: Crystallographic parameters and refinement data for complex **1**.

Empirical formula	$C_{60}H_{72}N_3O_3Pd_3Se_3$
Formula weight	1439.28
CCDC Number	2283578
Crystal habit, colour	Block, brown
Crystal size, mm^3	0.35 × 0.33 × 0.31
Temperature, *T*	100.00(13)
Wavelength, λ (Å)	0.71073
Crystal system	triclinic
Space group	'P -1'
Unit cell dimensions	a = 14.0778(3) Å b = 15.5286(3) Å c = 31.7803(4) Å α = 79.8730(10)°, β = 77.5150(10)° γ = 64.584(2)°,
Volume, V (Å^3)	6099.4(2)
Z	4
Calculated density, mg·m^{-3}	1.567
Absorption coefficient, μ (mm^{-1})	2.709
F(000)	2868
θ range for data collection	2.6250° to 28.5460°
Limiting indices	$-16 \leq h \leq 16$, $-18 \leq k \leq 16$, $-37 \leq l \leq 37$
Reflection collected/unique	41832/21485 [R(int)= 0.0443]
Completeness to θ	99.9% (θ = 24.999°)
Max. and min. transmission	0.28840/1.00000
Refinement method	'SHELXL-2018/3 (Sheldrick, 2018)'
Data/restraints/parameters	21485/0/1333
Goodness–of–fit on F^2	1.045
Final R indices [I>2sigma(I)]	$R1$ = 0.0473, $wR2$ = 0.1126
R indices (all data)	$R1$ = 0.0594, $wR2$ = 0.1192
Largest diff. peak and hole	1.67 and -1.54 e·Å^{-3}

Table S3. Statistical measures and Weibull distribution results of the I_{SET} and I_{RESET} currents of different memristor devices.

	Cu top electrode devices		**Al top electrode devices**	
Parameters	I_{RESET}	I_{SET}	I_{RESET}	I_{SET}
Mean	203 mA	435 mA	241 mA	368 mA
Weibull Shape Factor (β)	4.8 & 29.2	22.7	24.7	55.7

Table S4: Performance comparison of complex **1** as a memristor material with previously reported results for various molecular metal complexes found in the literature.

Molecular Material	**RS type**	**RS Mechanism**	**Memory type**	**Endurance (cycles)**	**Retention (s)**	**SET/ RESET Voltage**	**Energy Cost/ spike**	**Synaptic Actions/ Pattern Recognition**
Ru complex[1]	Digital	Proton conduction	RAM*	--	--	+ 1.5 V/ − 1.5 V	--	No/No
Iridium(III) complex[2]	Analog	Interplay of charge transfer and redox activities	RAM	--	2000	+ 0.8 V/ − 1.2 V		Yes/No
Aluminum(III) (Alq3) complex[3]	Digital	Filamentary	WORM*	--	10000	+ 4 V/ --	--	No/No
Alkynylgold(III) complex[4]	Digital	Filamentary	WORM	--	10000	± 5 V/ --	--	No/No
Platinum(II) complex[5]	Digital	Filamentary	WORM	--	10000	± 5 V/ --	--	No/No
Ni(II)-tetraaza[14]annulene complex[6]	Digital	Redox reaction modulated	RAM	500	18000	+1.5 V/ − 1.5 V	~ 100 μJ	No/No
Binuclear diradical cobalt(III) complex[7]	Analog	Ligand centred redox events	RAM	150	1200	− 1.0 V/ + 1.0 V	--	No/No
Azo anion diradical complexes of Rh(III)[8]	Digital	Schottky barrier modulated	RAM	> 15	>100	+ 2.75 V/ − 2.05 V	--	No/No
Pd^{II}_3 complex *	Analog	Redical centred redox activities and spin-polarized electronic transmission	RAM	> 1300	> 2100	+ 1.0 V/ − 1.0 V	7.63 nJ	Yes/Yes

$^+$ RAM – Random Access Memory and WORM – Write Once Read Many. * This work

Supporting References

1. Y. Hiruma, K. Yoshikawa and M. Haga, *Faraday Discussions*, 2019, **213**, 99–113.

2. Y. Zhuang, Y. Wang, Y. Deng, F. Li, X. Chen, S. Liu, Y. Tong and Q. Zhao, *Inorg. Chem.*, 2021, **60**, 13021–13028.

3. C.-L. Wong, M. Ng, E. Y.-H. Hong, Y.-C. Wong, M.-Y. Chan and V. W.-W. Yam, *J. Am. Chem. Soc.*, 2020, **142**, 12193–12206.

4. V. K.-M. Au, D. Wu and V. W.-W. Yam, *J. Am. Chem. Soc.*, 2015, **137**, 4654–4657.

5. A. K.-W. Chan, M. Ng, Y.-C. Wong, M.-Y. Chan*, W.-T. Wong and V. W.-W. Yam, *J. Am. Chem. Soc.*, 2017, **139**, 10750–10761.

6. A. Sławek, L. Alluhaibi, E. Kowalewska, G. Abdi, T. Mazur, A. Podborska, K. Mech, M. Marciszko-Wiąckowska, A. Maximenko and K. Szaciłowski, *Adv. Electron. Mater.*, 2024, 2300818.

7. S. Sinha, M. S. E, R. Mondal, S. Das, L. T. Manamel, P. Brandão, B. de Bruin, B. C. Das and N. D. Paul, *J. Am. Chem. Soc.*, 2022, **144**, 20442–20451.

8. N. D. Paul, U. Rana, S. Goswami, T. K. Mondal and S. Goswami, *J. Am. Chem. Soc.*, 2012, **134**, 6520–6523.

Optimized coordinates of complex 1

scf done: -3125.111836

Pd	9.059138	2.532369	11.032437
Pd	9.333601	5.294820	8.709021
Pd	6.127564	3.721684	9.290223
Se	7.216991	1.544349	9.659340
Se	10.484427	3.111077	9.106593
Se	7.532809	4.344234	7.318835
O	8.156668	2.250836	12.894056
O	10.622287	6.469112	9.857530
O	4.986969	5.468048	9.337221
N	4.895772	3.257766	10.848913
N	8.469575	7.115947	8.400498
N	10.547776	3.258049	12.224287
C	5.897782	1.064008	11.044203
C	4.845233	1.968446	11.365879
C	10.142335	7.678733	10.002991
C	5.957126	-0.214972	11.602412
H	6.802119	-0.867972	11.359069
C	4.214549	4.360470	11.314057
C	6.842145	6.142237	6.898865

C	11.807713	3.541879	11.709919
C	10.789857	8.641252	10.858643
C	8.845062	2.837715	13.839408
C	7.490579	7.293380	7.430150
C	8.929319	8.062572	9.288388
C	10.119061	3.472692	13.514835
C	4.248591	5.511928	10.417453
C	8.367047	2.872029	15.199342
C	4.931393	-0.664254	12.447014
H	4.982900	-1.664869	12.888260
C	5.785914	6.253208	5.991480
H	5.286541	5.345719	5.635590
C	8.305262	9.306254	9.576686
H	7.330340	9.514182	9.144134
C	12.106630	8.283325	11.567600
C	10.779007	4.266313	14.492181
H	11.648910	4.845259	14.194626
C	11.959560	3.649004	10.297534
C	7.130246	8.552092	6.871514
H	7.698084	9.441641	7.149444
C	10.151973	9.864834	11.039488
H	10.617123	10.596852	11.702026
C	13.175578	7.883699	10.521604
H	12.848040	7.014044	9.934028
H	14.120838	7.620946	11.031748
H	13.376096	8.725464	9.833373
C	3.771606	1.456261	12.147543
H	2.882783	2.070514	12.301414
C	9.104948	3.614625	16.115603
H	8.744040	3.671251	17.144077
C	12.987751	3.666334	12.496483
H	12.941503	3.453509	13.565812
C	3.551794	4.462895	12.567171
H	3.653063	3.648536	13.279453
C	13.175893	4.022912	9.720904
H	13.242425	4.132551	8.633197
C	3.466321	6.679161	10.739091
C	5.385106	7.514299	5.526876
H	4.552358	7.599632	4.821282
C	10.288099	4.347222	15.788873
C	3.823556	0.167534	12.681103
H	2.982416	-0.194755	13.282714
C	6.091740	8.654744	5.944841
H	5.835474	9.639264	5.537739
C	11.312851	4.312588	18.087322

H	10.419305	3.837171	18.527599
H	11.795503	4.916205	18.878246
H	12.011474	3.510342	17.788451
C	7.063380	2.151003	15.580309
C	14.303548	4.233757	10.527316
H	15.254013	4.533118	10.073906
C	8.899226	10.212526	10.445700
C	2.791197	6.678828	11.955818
H	2.212235	7.563903	12.225246
C	14.206356	4.013409	11.911809
H	15.094993	4.105997	12.546181
C	10.955851	5.206583	16.874587
C	2.839833	5.607934	12.901145
C	11.849479	7.104494	12.537529
H	11.102174	7.385139	13.302284
H	12.788632	6.829088	13.051578
H	11.479294	6.221806	11.997728
C	7.166720	0.649994	15.216054
H	6.227127	0.132431	15.484369
H	7.995101	0.173824	15.772377
H	7.338064	0.515594	14.138494
C	12.662655	9.463708	12.388035
H	12.871653	10.345133	11.754889
H	13.612632	9.160602	12.862973
H	11.972572	9.770124	13.195019
C	3.438888	7.881388	9.779988
C	2.498900	8.997335	10.276811
H	1.456125	8.645309	10.377622
H	2.502540	9.826659	9.547385
H	2.822704	9.410972	11.249120
C	0.625531	6.071065	14.004254
H	0.150012	5.243150	13.447973
H	0.478631	6.998055	13.423402
H	0.095561	6.191396	14.967362
C	2.124717	5.773329	14.251916
C	12.248687	5.881598	16.378395
H	12.995177	5.137942	16.045681
H	12.701539	6.465678	17.199093
H	12.054934	6.574604	15.542344
C	4.866686	8.470684	9.672120
H	4.866417	9.334739	8.982436
H	5.575456	7.723527	9.288781
H	5.221789	8.813606	10.661289
C	5.887142	2.803165	14.813458
H	6.031862	2.725850	13.726940

H	5.795995	3.872590	15.078158
H	4.939971	2.296694	15.075142
C	2.767344	6.953298	15.021787
H	2.688778	7.899569	14.458322
H	3.838772	6.757658	15.208148
H	2.264994	7.096849	15.996710
C	2.945826	7.428831	8.384163
H	1.920770	7.019859	8.450784
H	3.608621	6.660611	7.960758
H	2.929810	8.291796	7.692935
C	6.764769	2.253992	17.088898
H	5.831682	1.707073	17.312610
H	6.620193	3.300462	17.413406
H	7.569325	1.807248	17.700953
C	8.249673	11.558206	10.806712
C	2.224969	4.510941	15.129147
H	1.676661	4.670637	16.074467
H	3.270832	4.271534	15.385646
H	1.781175	3.630925	14.629572
C	9.230337	12.707652	10.468312
H	8.776695	13.684016	10.720959
H	9.474920	12.707414	9.390731
H	10.176337	12.622650	11.030568
C	9.968494	6.313646	17.319200
H	9.702402	6.962307	16.465156
H	10.424270	6.943482	18.105958
H	9.034140	5.888328	17.725605
C	7.934068	11.575353	12.322696
H	7.470583	12.537926	12.609207
H	8.846111	11.444799	12.931154
H	7.233672	10.761198	12.582632
C	6.938014	11.802843	10.036478
H	6.175002	11.042091	10.273493
H	7.100577	11.800790	8.943531
H	6.523946	12.789183	10.311179